Aerosol and Air Quality Research, 17: 1281–1293, 2017

ISSN: 1680-8584 print / 2071-1409 online
doi: 10.4209/aaqr.2016.08.0369

Performance and Uncertainty in Measuring Atmospheric Plume Opacity Using Compact and Smartphone Digital Still Cameras

Wangki Yuen[1], Yichao Gu[1], Yalin Mao[1], Sotiria Koloutsou-Vakakis[1], Mark J. Rood[1*], Hyun-Keun Son[2], Kevin Mattison[3], Bill Franek[3], Ke Du[4]

[1] *Department of Civil and Environmental Engineering, University of Illinois at Urbana-Champaign, IL 61801, USA*
[2] *Department of Environment and Health, Kosin University, Busan, Korea*
[3] *Illinois Environmental Protection Agency, IL 62702, USA*
[4] *Schulich School of Engineering, University of Calgary, Alberta T2N 1N4, Canada*

ABSTRACT

Quantification of visible ambient plume opacity measurements using compact and smartphone digital still cameras (DSCs), and Digital Optical Method (DOM) are evaluated here. A new camera calibration method that employs exposure value compensation in place of exposure time or radiance of a surface is described and evaluated. This new and simpler method allows an automatic exposure controlled DSC to be calibrated using its own DSC settings. We also test the use of color in place of grayscale pixel values (PVs) to measure opacity. Finally, we determine the uncertainty of the opacity measurements. Two compact DSCs and two smartphone DSCs are tested to measure plume opacity values of smoke generated with an outdoor smoke generator, in comparison to the plume opacity values measured with an in-stack transmissometer. Results show that: 1) smartphone DSCs, like compact DSCs, can pass opacity measurement requirements set by USEPA; 2) the new simpler calibration method generates values within 5% in opacity on average compared to opacity values from the reference transmissometer; 3) non-uniform background color dominates the uncertainty of opacity measurements, and such uncertainty is wavelength dependent; and 4) the diffusive scattering parameter, used in DOM's transmission model, is lower for black plumes than white plumes, and is wavelength dependent. These results improve our understanding of using DSCs and the parameters that introduce uncertainty to DOM to improve measurements of plume opacity that can improve protection of human health.

Keywords: Pixel values; Digital Optical Method; Transmissometer; RGB; Exposure values.

INTRODUCTION

Technological advances have made possible the development of low-cost environmental sensors that are portable, and offer ability for rapid acquisition, transmission, storage, and analysis of data (Snyder *et al.*, 2013). Questions have arisen regarding the accuracy of such methods compared to traditional standard methods (Nieuwenhuijsen *et al.*, 2015; Reis *et al.*, 2015). We present here results from using such method for monitoring plume opacity. Opacity is defined as the percent of visible light attenuated by a plume. Opacity relates to particulate matter (PM) concentration in plumes because PM is typically the most significant contributor of visible light attenuation. Measuring PM is important because it is an air pollutant that causes adverse health effects (Dockery and Pope, 1994; Pope and Dockery, 2006), reduces visibility (Malm, 1999; Watson, 2002), and affects climate (Anenberg *et al.*, 2012). PM is regulated by the United States Environmental Protection Agency (USEPA) as a criteria air pollutant under the 1990 Clean Air Act Amendments (USEPA, 2016). The World Health Organization (WHO) also has established Air Quality Guidelines (WHO, 2006) for PM that provide an international reference for countries to set ambient air quality standards (Vahlsing and Smith, 2012). United States (US) legislation mandates opacity measurements at select industrial facilities to monitor emitted pollution (40 CFR Part 60, USEPA, 1993). Each US state may also have separate opacity standards specified in their State Implementation Plans (USEPA, 1993). USEPA promulgated Method 9 in 1974 for opacity evaluation, which specifies using human observers to measure plume opacity (USEPA, 1993). Drawbacks of Method 9 are subjective opacity readings by humans and difficulty to provide archival digital records of opacity readings and the environment, such as meteorology or observational background during the measurement (Du *et*

[*] Corresponding author.
Tel.: 1-217-333-6963; Fax: 1-217-333-9464
E-mail address: mrood@illinois.edu

al., 2007). To resolve these issues, digital still cameras (DSCs) were evaluated and approved by American Society of Testing Materials (ASTM) as an appropriate technique to measure plume opacity values (ASTM Standard D7520, 2016). Besides the US, Canada regulates opacity from electricity generation sources (Environment and Climate Change Canada, 2010). Thailand also regulates opacity emitted from select sources, using measurement methods based on the USEPA Method 9 (Pollution Control Department, 2004). Other applications of DSCs in monitoring air quality include measurements of concentrations of black carbon (Du *et al.*, 2011; Ramanathan *et al.*, 2011), fugitive PM emissions (Du *et al.*, 2013), gaseous air pollutants such as ozone (Hasenfratz *et al.*, 2012) and visibility monitoring (Poduri *et al.*, 2010).

Digital Optical Method (DOM) was developed to measure ambient plume opacity values with DSCs (Du *et al.*, 2007). DOM can be implemented using either the contrast or the transmission models. The contrast model requires the digital image to contain a plume that passes in front of and near two contrasting backgrounds. The transmission model requires the digital image to contain a plume that passes in front of and near one background that is in contrast to the plume. In the transmission model, the contrast between the plume and its background is parametrized by using a diffusive scattering parameter (K). DSCs are calibrated to relate amount of light exposure to pixel value (PV). Previously, compact DSCs were calibrated either by varying their exposure time for manual exposure controlled DSCs, or by varying the surface radiance of the same image for automatic exposure controlled DSCs (Du, 2007). Average PVs are measured at several regions in an image and are used to determine the amount of exposure and then opacity.

Smartphones have become ubiquitous and provide additional desirable capabilities for monitoring plume opacity. Such capabilities could include software adaptation as a smartphone application, internet connectivity, and potential for crowdsourcing of plume opacity measurements. Thus, smartphone DSCs could be deployed for community monitoring of plume opacity values. Given the capabilities of smartphone technology, it is important to investigate how such technology can be used to obtain reliable opacity measurements.

This research improves our knowledge of using compact and smartphone DSCs in three areas. First, a simpler alternative calibration method is evaluated. This does not require another calibrated DSC to calibrate automatic exposure controlled DSCs. Second, the effects of background color on measured opacity values are quantified. This is important because color contrasts between background(s) and plumes affect opacity measurement uncertainty. Third, the sources of uncertainty in the opacity measurements are identified, and their relative importance is quantified. Uncertainties of measured opacity values are determined using error propagation of DOM models. Such uncertainty evaluation describes the factors that affect uncertainty of opacity measurements, which are important for better decision in choosing appropriate environmental conditions for opacity measurements. Overall, these contributions increase the applicability and confidence in using DOM to measure plume opacity at non-ideal conditions, which encourages community monitoring of PM.

METHODS

Two compact DSCs (Sony Cybershot DSC-P100 (Sony A) and Sony Cybershot DSC-S30 (Sony B)) and two smartphone DSCs (Samsung GT-S5360 (Samsung) and Nokia E61i (Nokia)) were used during the field campaign. Both compact DSCs are manual-exposure controlled, and both smartphone DSCs are automatic-exposure controlled. Exchange Image File Format (EXIF) data from these DSCs are available in Table S1 of Supporting Information.

Camera Calibration

Camera calibration determined the relationship between exposure and PVs in a particular DSC, known as the response curve. Grayscale PV was calibrated by varying exposure time (ET method) for manual exposure controlled DSCs, and varying surface radiance (SR method) for automatic exposure controlled DSCs (Du, 2007). The ET method involves taking pictures of the same white surface, with the DSC's aperture size fixed and exposure time setting varied from 1/500 to 2 sec for 15 settings. Average PV is measured at the center of the each picture's white surface, with a sample size of 700 pixels by 500 pixels. A regression is then fit for ln(exposure time) against ln(PV), and the coefficients characterize the response curve of the DSC. Since exposure is proportional to exposure time, and DOM only requires relative exposure (ratio of exposure) between any two regions, exposure time is used as a proxy of relative exposure (Du, 2007). The SR method involves a calibrated manual exposure controlled DSC, an un-calibrated automatic exposure controlled DSC, and a checkerboard with twelve different shades of gray. The manual exposure controlled DSC is the reference for the SR method. The two DSCs are placed next to each other and each takes a digital image of the checkerboard. The average PV is obtained for each DSC within the center of each of twelve squares, typically 30 pixels by 30 pixels. PVs measured by the calibrated DSC are converted to the amount of relative exposure, based on exposure time. A quadratic regression is then fitted for ln(relative exposure) of the calibrated DSC against ln(PV) of the un-calibrated DSC, similar to the ET method.

The SR method requires an additional calibrated DSC to calibrate automatic exposure controlled DSCs. Therefore, we developed and tested the new exposure value compensation method (EC) to calibrate automatic exposure controlled DSCs as an alternative to the SR method. Automatic exposure controlled DSCs typically allow compensating exposure values (EVs) using DSC settings. Each addition of one EV means doubling the exposure. This property allows obtaining the camera response curve by using the DSC settings and a white surface, without using a calibrated DSC. The EC method is similar to the ET method in that a DSC takes digital images of a white surface by varying the EV compensation, from –2 to +2 for 13 settings. An average PV for each digital image is determined as with the ET method. The quadratic fit procedure is also used, except $\ln(2^{EV})$ against ln(PV) is plotted because of the relationship of EV to exposure. The calibrations were performed with grayscale PVs and with Red-Green-Blue (RGB) PVs, resulting to four response curves for each DSC. These four curves were then used to quantify opacity values.

DSCs were calibrated with more than one method to compare the effect of calibration methods on measuring plume opacity. Sony A was calibrated by EC and ET methods, while Sony B was calibrated by the EC, ET, and SR methods. Both smartphone DSCs were only calibrated by the SR method because settings for changing exposure time and EV compensation are not available with these DSCs. The ET response curve for Sony A was used to calibrate Sony B and the two smartphone DSCs through the SR method. We performed three replicates of calibrations for each calibration method and DSC combination. The replicates were used to characterize the effect of calibration uncertainty on opacity measurement uncertainty. The resulting fitted coefficients for each DSC, color, and calibration methods are provided in Table S2 of Supporting Information.

Field Campaign and Opacity Calculation

Calibrated DSCs were field tested in July 2013 in Springfield, IL, USA, during a daytime Illinois EPA visible emission evaluation course (Illinois EPA, 2015). A smoke generator produced black or white plumes from an elevated stack. A white-light transmissometer in the stack monitored plume opacity at 15 Hz and was the reference for comparison with DSC measured opacity values. During the visible emission evaluation course, DSCs observed plumes with the sun within 140° sector behind the DSCs, as per Method 9 and ASTM requirements (ASTM, 2013). All DSCs were 20 m from the smoke generator. Two different pairs of existing contrasting backgrounds were tested for black plumes and white plumes using the contrast model. The first background pair was a dark gray roof and the white (cloudy) sky. The second background pair was a red sign background and the white sky. In addition, we tested a single white sky background using the transmission model for black plumes only. The statistics of grayscale and RGB PVs for the dark gray roof, the white sky, and the red backgrounds, measured by Sony B with EC calibration, are shown in Table S3 of Supporting Information to justify the use of these color designations. Examples of digital images for such backgrounds are shown in Fig. S1 of Supporting Information.

The contrast model calculates plume opacity using two contrasting and co-located backgrounds. Four regions are selected in each digital image: two regions with a bright background with and without the plume in front of the backgrounds, and two regions with a dark background with and without the plume in front of the backgrounds. PVs within each of the four regions are determined and then averaged arithmetically. The average PVs in each region are then converted into amounts of relative exposure using the response curve for the respective calibrated DSC. The calculation to determine opacity values assumes that the light attenuation by the aerosol between the DSC and the plume is insignificant, which was verified previously (Du, 2007). Opacity is calculated using Eq. (1) (Du *et al.*, 2007):

$$O_c = 1 - \frac{\dfrac{E_{wp}}{E_w} - \dfrac{E_{bp}}{E_w}}{1 - \dfrac{E_b}{E_w}} \tag{1}$$

where: O_c = plume opacity using contrast model; E_{wp} = amount of exposure caused by the bright background with plume; E_w = amount of exposure caused by the bright background without plume; E_{bp} = amount of exposure caused by the dark background with plume; and E_b = amount of exposure caused by the dark background without plume.

The transmission model calculates plume opacity using one background that is in contrast to the plume. Average PVs are measured at areas of background with the plume in front of and next to the background. The average PVs of each of the two regions are then converted to relative exposure using the camera response curve of a specific DSC. Opacity is calculated using Eq. (2) (Du *et al.*, 2007):

$$O_t = \frac{1 - \dfrac{E_p}{E}}{1 - K} \tag{2}$$

where: O_t = plume opacity using transmission model; E_p = amount of exposure caused by the background with plume; E = amount of exposure caused by the background without plume; and K = diffusive scattering parameter. K is defined as:

$$K = \frac{\omega}{4\pi I_{np}(\theta = 0)}\left(\int_0^{2\pi}\int_{-1}^{1} I_{bg}(\theta')P(\theta')d\mu' d\phi' + P(\theta_S)S_0 e^{-\frac{\tau}{\mu_0}}\right) \tag{3}$$

where: ω = single scattering albedo of the plume; $I_{np}(\theta = 0) = I_{bg}(\theta = 0)$ = radiance of background light pointing at the referenced path; $I_{bg}(\theta)$ = radiance of background light at angle θ from the referenced path; P(θ) = scattering phase function of the plume at angle θ from the referenced path; μ = cos (zenith angle); ϕ = azimuth angle; $P(\theta_s)$ = scattering phase function at angle between the sunlight and the referenced light path (θ_s); S_0 = solar constant = 1360 W m^{-2} T = optical depth of background atmosphere; and μ_0 = cos (solar zenith angle).

Inside the parentheses, the first term relates to the diffuse scattering of the background, and the second term relates to the direct solar radiation. Du (2007) also shows that when K = 1, the radiances of the plume and the background are equal, thus lacking contrast. Using Eq. (3), K was calculated to be 0.16 for a black plume in front of a blue sky, and 1.43 for a white plume in front of a blue sky (Du, 2007). Using the same method described by Du (2007), K was calculated to be 0.14 for a black plume in front of a white (overcast) sky background. K for a white plume against a white overcast was not calculated because of lack of contrast between the plume and the background colors, but such K should be 1 in theory. Since the K calculation method provided by Du (2007) requires assumptions of particle properties and models that simulate the radiance distribution of background light, we here used an empirical method to obtain K, which is described in the section "Analysis of Diffusive Scattering Parameter (K)" below. The empirical K values will be compared by the theoretical K values above.

Opacity Measurement Performance Metrics

The individual opacity errors (IOEs) and average opacity errors (AOEs) were calculated to evaluate the quantification of opacity values by the DSCs as defined by Method 9. IOE and AOE are defined as follows:

$$\mathrm{IOE} = \left|O_{c,i} - O_{t,i}\right| \tag{4}$$

where: $O_{c,i}$ = ith individual opacity measured by DSC and $O_{t,i}$ = ith individual opacity measured by transmissometer (reference signal).

$$\mathrm{AOE} = \frac{1}{N}\sum_{i=1}^{N}\left|O_{c,i} - O_{t,i}\right| \tag{5}$$

where: N = the total number of individual measurements in a set for a plume type.

Human observers are certified to measure plume opacity if the maximum IOE does not exceed 15% in opacity and AOE does not exceed 7.5% in opacity for black and white plumes during a test sequence (Method 9, USEPA, 1993). Using these criteria, DOM has been successfully tested with grayscale PV measurements (Du *et al.*, 2007). In this research, these criteria will be tested on grayscale and RGB PVs.

Uncertainty Analysis

Uncertainty of opacity values can be due to two reasons: uncertainty in camera calibration and uncertainty due to the non-uniformity of the background colors, as quantified by PVs. The former relates to DSC hardware uncertainty, while the latter relates to conditions external from the DSCs. To determine the uncertainty due to camera calibration, we calculated amounts of relative exposure due to plume opacity value three times, using DOM models and the three replicate camera calibrations that were mentioned previously. The greatest opacity absolute difference resulting from the three response curves was treated as uncertainty and reported.

In both DOM models, backgrounds are assumed to be uniformly colored, which means the standard deviation of PVs within a select region is zero. However, such condition is challenging to achieve in the ambient environment. To determine the uncertainty due to non-uniformity of the background colors, the standard deviation of PVs was determined for each background first. To do so, a color image that includes a plume in front of and next to two contrasting backgrounds was selected. Four regions in the picture describing the backgrounds, defined by the contrast model, were randomly selected ten times, using random dimensions of rectangles (typically with sizes between 10 pixel × 10 pixel and 30 pixel × 30 pixel, within a 50 pixel × 50 pixel area). These four regions have average PVs between 75 and 200. The standard deviations of the PVs for these replicates for each background region were calculated. The results showed that the standard deviations ranged from 0.3 to 2.1 PV and coefficients of variations (COVs, (standard deviation/mean) × 100%) from 0.4% to 1.8%. For the pictures from our field experiment, the maximum PV standard deviation occurs at the dark gray roof region with plume present, where the edges of tiles on the roof introduce non-uniform color. Next, measured mean PVs of the select regions in other digital images were increased or decreased by a PV deviation of 2 because this was the maximum standard deviation determined in the background PV standard deviation tests that is explained above, rounded to an integer because PVs can only be set as integer values. Uncertainties of exposures (δEs) in each of the select regions in a digital image were then calculated by determining the difference in E between the measured PVs, with and without PV deviation, using the camera response curve. Opacity uncertainties were then calculated by using error propagation (Bevington and Robinson, 2002) on Eqs. (1) and (2) and δEs, assuming that the measured quantities are independent of each other. The opacity uncertainty for the DOM contrast model (δO_c) results in:

$$\delta O_c = \left|\frac{1}{E_w - E_b}\right|\sqrt{\left(\delta E_{wp}{}^2 + \delta E_{bp}{}^2\right) + \left(1 - O_c\right)^2\left(\delta E_w{}^2 + \delta E_b{}^2\right)} \tag{6}$$

while the opacity uncertainty for the transmission model (δO_t) results in:

$$\delta O_t = \left|\frac{1}{1-K}\right|\sqrt{\left(\frac{E_p}{E}\right)^2\left[\left(\frac{\delta E_p}{E_p}\right)^2 + \left(\frac{\delta E}{E}\right)^2\right] + \left(O_t \delta K\right)^2} \tag{7}$$

where δO_c and δO_t describe the uncertainties of O_c and O_t in Eqs. (1) and (2), respectively. The uncertainty of the K (δK) was determined empirically by the standard deviation of K (see section "Analysis of Diffusive Scattering Parameter (K)" below). Eq. (6) indicates that when the two contrasting backgrounds lack contrast, $E_w - E_b$ approaches zero and opacity uncertainty approaches infinity. Similarly, Eq. (7) indicates that when K approaches to 1, which happens when the plume and the background lack contrast, opacity uncertainty also approaches infinity. Increasing contrast between two backgrounds, or between a background and a plume, is therefore needed so that uncertainty of opacity value decreases. Both positive and negative deviations by 2 PV were tested, but since positive deviations differ from negative deviations by < 0.3% opacity for all grayscale and RGB measurements, only results with positive deviations are shown in the section "Results and Discussion".

Analysis of Diffusive Scattering Parameter (K)

To empirically obtain K for select background and plume color combinations, we first calculated the plume opacity using two contrasting backgrounds and the contrast model (Eq. (1)). Then, for each DSC, we used the transmission model (Eq. (2)), opacity values from the contrast model, and the one background that was in contrast to the plume to back-calculate K. Means and standard deviations of K were calculated and are reported, by each background-plume color combination, and by grayscale and RGB PV values. Before calculating the statistics of K, outliers were identified by using 1.5 times inter-quartile range of all the K data in each category, and were removed (Montgomery and Runger, 2011). These outliers are possibly caused by unknown random errors introduced by, for instance, fast changing micrometeorological conditions that can alter the plume direction and turbulent dispersion.

RESULTS AND DISCUSSION

Number of pictures taken by each DSC, for each background type and plume color, are shown in Table S4 of the Supporting Information. Although we aimed to obtain at least 25 digital images for each DSC in each measurement condition due to Method 9 requirements, some DSCs using red background and white sky have less than 25 digital images because of the short window of measurement period for this condition.

Opacity Measurement Performance

The comparisons between opacity measurements of DSCs and the transmissometer in grayscale, using the dark gray roof and white sky as the contrasting background pair, are shown in Figs. 1(A) and 1(B). Box plots that summarize the IOE data in grayscale for each compact or smartphone DSC and each plume color using the same background pair are shown in Figs. 1(C) and 1(D). When using this background pair, both compact DSCs and both smartphone DSCs passed Method 9 criteria for black and white plumes.

The comparisons between opacity values measured by the DSCs and transmissometer in grayscale, using the white sky as the only background and transmission model for black plume only, are shown in Fig. 2(A). We did not use the transmission model for white plumes with the white sky background due to the lack of sufficient contrast between the white plumes and white sky background. The box plot that summarizes the IOEs for black plumes in grayscale, for opacity values measured by each compact or smartphone DSC using transmission model compared to transmissometer values, is shown in Fig. 2(B). The results show that all four DSCs passed the Method 9 AOE and IOE requirements.

The comparisons between opacity measurements of DSCs and transmissometer in grayscale, using red background and white sky as the contrasting background pair, are shown in Fig. 3(A) for black plume and 3(B) for white plume. Box plots that summarize the IOE data for each compact or smartphone DSC, using the same background pair, are shown in Fig. 3(C) for black plume and 3(D) for white plume. In contrast with the dark gray roof and sky background pair for black and white plumes (Fig. 1), AOEs for all DSCs are > 7.5% for white plumes using red background and white sky background pair. AOEs for the two smartphone DSCs are also > 7.5% for black plumes using red background and white sky background pair. From the data in Figs. 1 through 3, using the dark gray roof and white sky background pair produces more accurate opacity results than using the red background and white sky background pair. We expect that the results are due to background color, which will be further explained in the next section "Wavelength Dependence".

The comparison of box plots describing IOEs and AOEs among three calibration methods (EC, ET, and SR) for the Sony B DSC, when measuring plume opacity values with the contrast model for black and white plumes, using the dark gray roof and white sky background pair, are shown in Fig. 4. The new EC and the previous ET and SR methods result in AOEs (Eq. (5)) of 2.8%, 4.1%, and 2.6% in opacity, respectively, for black plumes, and 2.8%, 5.6%, and 3.4% in opacity, respectively, for white plumes, using grayscale PV measurements (Fig. 4). This shows that the new EC method yields opacity values similar to the previous SR calibration method, making the EC method possible as an alternative method to calibrate automatic exposure controlled DSCs. The effect of calibration method on opacity uncertainty is examined in the "Uncertainty Analysis" section.

Wavelength Dependence

The difference in performance of DOM due to background color has been demonstrated in Figs. 1 through 3. Since backgrounds can have a wide range of colors, this motivated us to look at the wavelength effect on the opacity measurements. The results may help making decisions regarding the choice of backgrounds to determine opacity values with DOM. For brevity, only comparison of plume opacity values measured by Sony B DSC's RGB PVs to that measured by the transmissometer, using two different background pairs, is shown in Fig. 5. A 1:1 line is shown to denote perfect agreement line. In Fig. 5(A) for white sky and dark gray roof background pair, opacity measured by red PV has an AOE of 6.5%. However, when looking at Fig. 5(B) that uses the red background and white sky background pair, measurements in red PV has a higher AOE (19.1% AOE). This is because red background and white sky backgrounds have less red contrast between these backgrounds compared to white sky and dark gray roof backgrounds. A red background reflects more red light but absorbs more green and blue light, while white sky reflects all visible light. This results in lower contrast between red and white sky backgrounds for red light than for blue or green light, and successively results in higher opacity uncertainty for red PV. Similar results are expected for green light and green background or blue light and blue background, but there were not available background in these colors to test for this field experiment.

We also observe in Fig. 5(A) that even when using a white sky and dark gray roof background pair, where PVs for red, green, and blue are the same, opacity measured by red PV tends to be lower than grayscale transmissometer

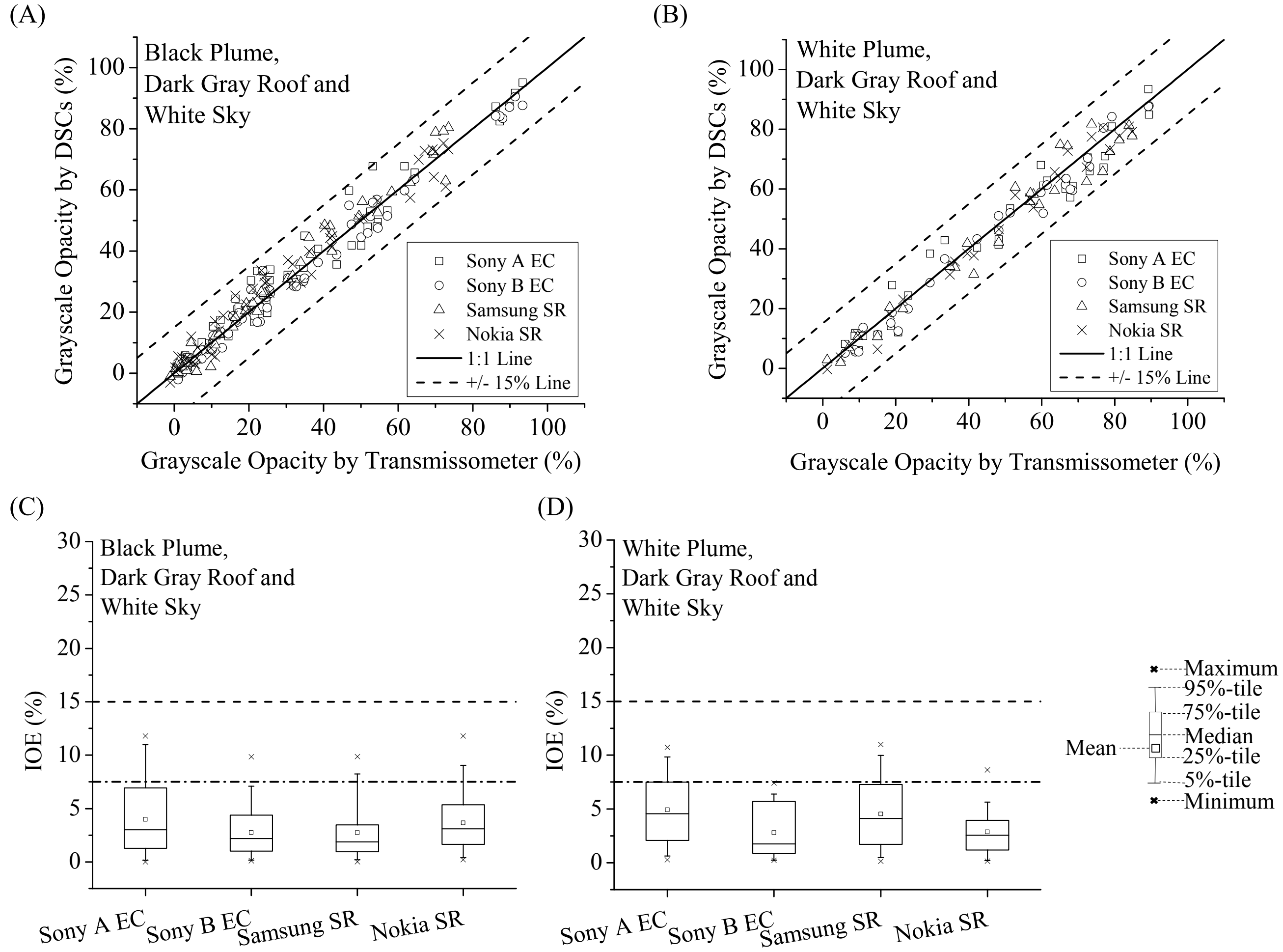

Fig. 1. Comparisons between opacity values measured by the DSCs and transmissometer using the contrast model, in grayscale, for (A) black plumes and (B) white plumes, using dark gray roof and white sky as the contrasting background pair. The 1:1 line shows perfect agreement in measurements. The ± 15% lines show the maximum IOE allowable for a DSC to pass the certification in measuring plume opacity. Box plots that summarize IOE and AOE results for each DSC are also shown for (C) black plumes and (D) white plumes.

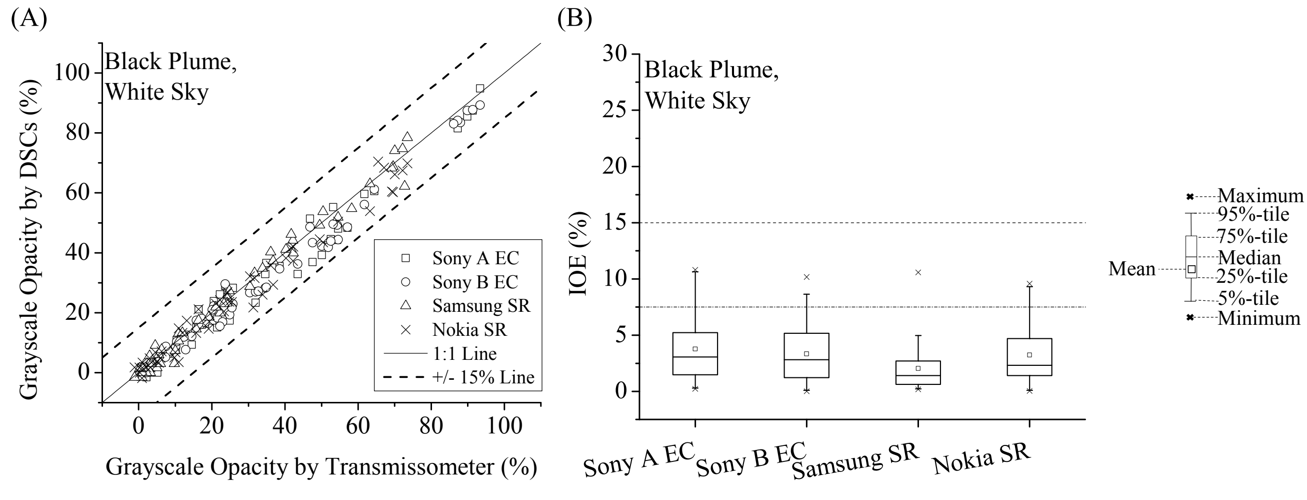

Fig. 2. (A) Comparisons between opacity measurements of DSCs and transmissometer using the transmission model, in grayscale, for black plumes and white sky background (K = 0.14). The 1:1 line shows perfect agreement in measurements. The ± 15% lines show the maximum IOE allowable for a DSC to pass the certification in measuring plume opacity. (B) Box plot that summarizes corresponding IOE and AOE results for each DSC, for black plumes and white sky background.

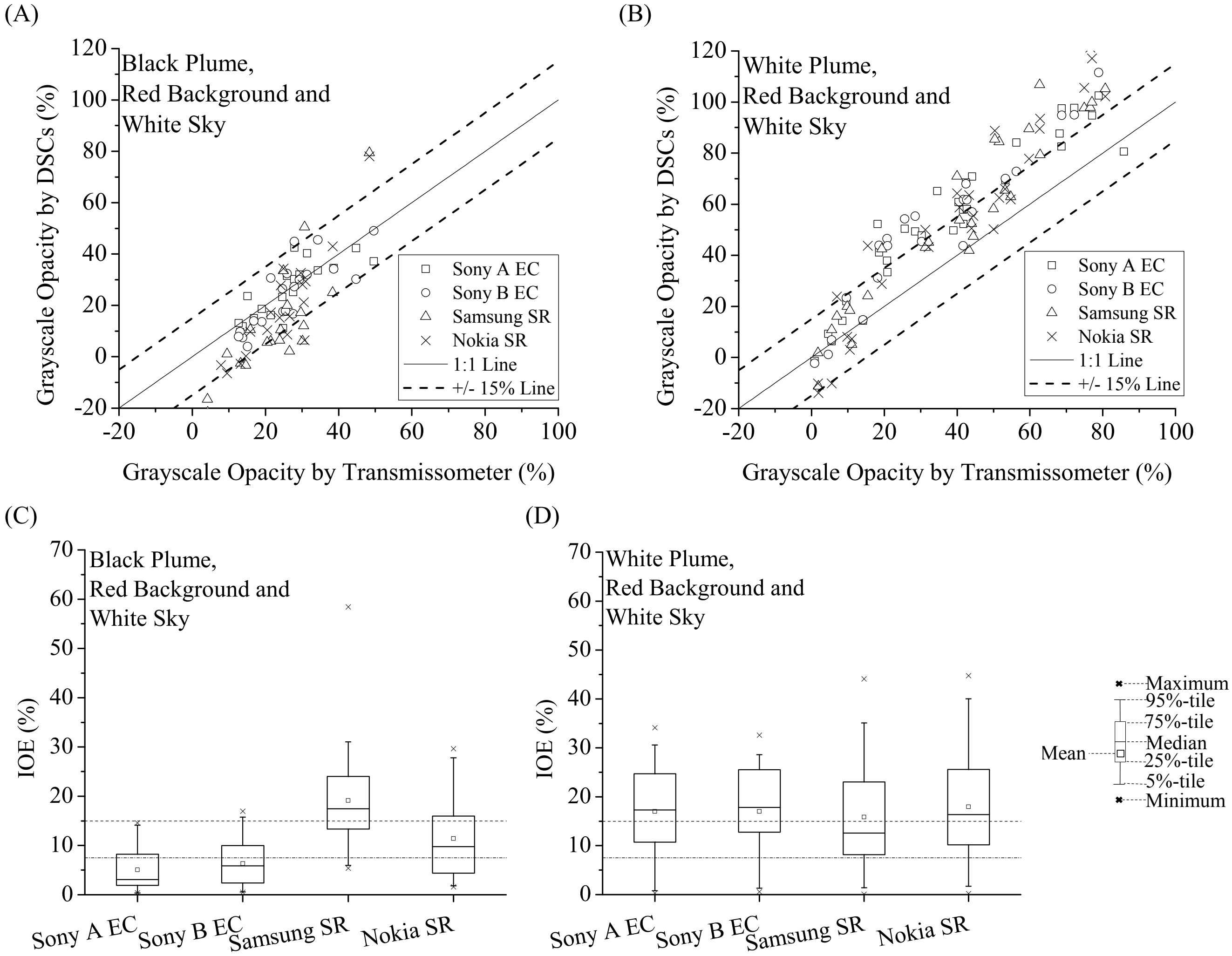

Fig. 3. Comparisons between opacity measurements of DSCs and transmissometer using contrast model, in grayscale, for (A) black plumes and (B) white plumes, using red background and white sky as contrasting background pair. The 1:1 line shows perfect agreement in measurements. The ± 15% lines show the maximum IOE allowable for a DSC to pass the certification in measuring plume opacity. Box plots that summarize IOE and AOE results for each DSC are also shown for (C) black plumes and (D) white plumes.

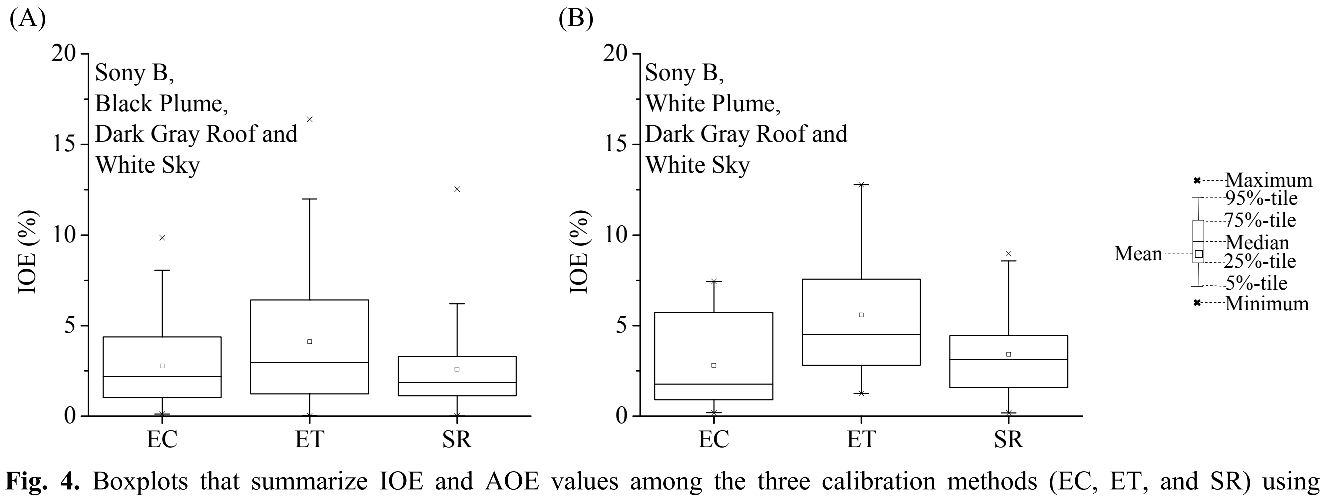

Fig. 4. Boxplots that summarize IOE and AOE values among the three calibration methods (EC, ET, and SR) using grayscale for Sony B DSC, and contrast model with dark gray roof and white sky background pair, for (A) black plumes and (B) white plumes.

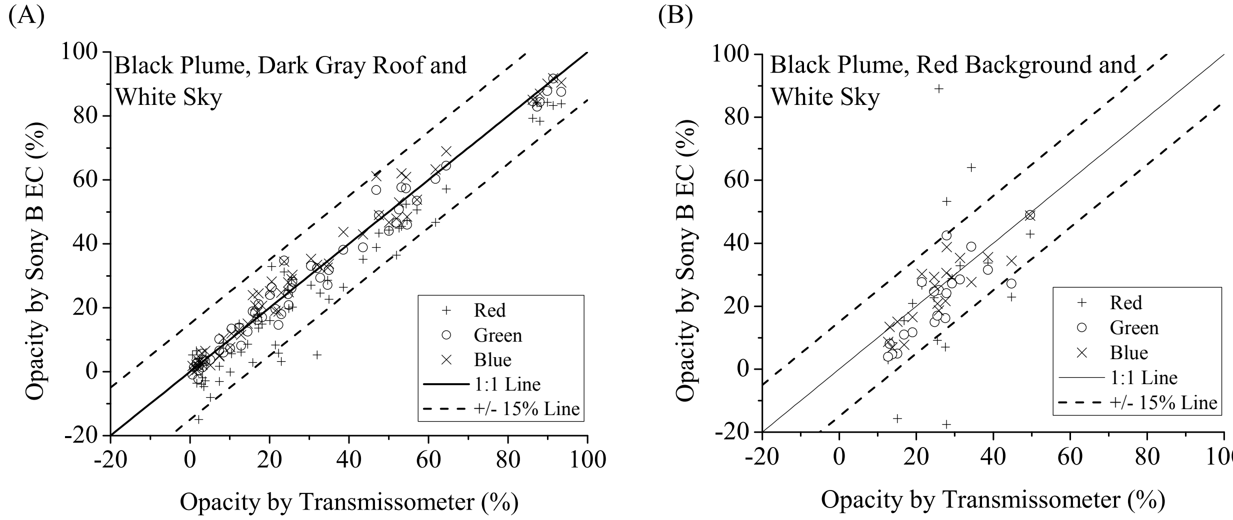

Fig. 5. Relationship of opacity measurements of Sony B DSC using RGB PVs to grayscale transmissometer measurements for black plumes using contrast model. Background pairs are (A) dark gray roof and white sky, and (B) red background and white sky.

measurements (by an average of 6.5% in opacity), while opacity measured by blue PV tends to be higher than grayscale transmissometer measurements (by an average of 1.2% in opacity). Opacity measured by green PV is only slightly lower than grayscale transmissometer measurements (by an average of 0.7% in opacity). Such similar trend is observed when the opacity values measured by RGB PVs are plotted against these values measured by grayscale PV (Supporting Information, Fig. S2). This happens because opacity depends on wavelength of light, as described by the Ångström equation (Ångström, 1964). The red PV results in the highest systematic error because Ångström equation is non-linear, and red has the longest wavelength. Such wavelength dependence of opacity was also observed by Conner and Hodkinson (1972). The results in Fig. 5(A) suggest that using DSCs' green or blue PV can be a substitute to grayscale PV in measuring plume opacity for black-and-white background pair, since opacity measured by green or blue PVs differ from opacity measured by grayscale PV by < 2%. Such results are also supported by the maximum IOEs and AOEs as compared to grayscale transmissometer measurements (maximum IOEs for red, green, and blue are 26.7%, 11.1%, and 14.3%, respectively. AOEs for red, green, and blue are 7.8%, 3.0%, and 3.0%, respectively). Such use of alternative light wavelengths is useful if backgrounds have higher contrast when using green or blue compared to grayscale. As mentioned before, higher contrast reduces the uncertainty of opacity measurements. For example, for Fig. 5(B), the average grayscale PV of the red background and the white sky background, measured by Sony B, are 42 and 157, respectively. However, the average green PV of the red background and the white sky background are 14 and 159, respectively. Thus, using green PV provides more contrast than using grayscale PV because the PV difference is 145 for the green wavelength, which is larger than 115 for the grayscale. Conversely, using red PV of the DSC to measure plume opacity is not recommended due to the highest systematic error in opacity measurements.

Uncertainty Analysis

The maximum absolute opacity differences of Sony B, Samsung, and Nokia, calculated from the triplicate response curves are shown in Table 1. The maximum considers the difference for all grayscale and RGB PVs. Results from Sony A are absent because replicates are not available. Results show that uncertainty due to camera calibration introduces < 2% opacity uncertainty.

The calculated uncertainty of DSC grayscale opacity measurement due to non-uniform background colors is shown in Fig. 6. The results are grouped between the two plume colors, and between two contrasting background pairs. The results show that uncertainty due to non-uniform

Table 1. Maximum absolute opacity differences among triplicate calibration curves that represent the uncertainty of opacity values due to calibration of the DSCs. The maximum considers the difference for all grayscale and RGB PVs.

Plume color	Background	Sony B EC (%)	Samsung SR (%)	Nokia SR (%)
Black	Dark gray roof and white sky	0.1	0.3	1.2
White	Dark gray roof and white sky	0.2	0.5	0.2
Black	White sky only	1.0	0.4	2.3
Black	Red background and white sky	0.1	0.4	1.2
White	Red background and white sky	0.1	0.3	2.0

* Sony A results are absent because replicates are not available.

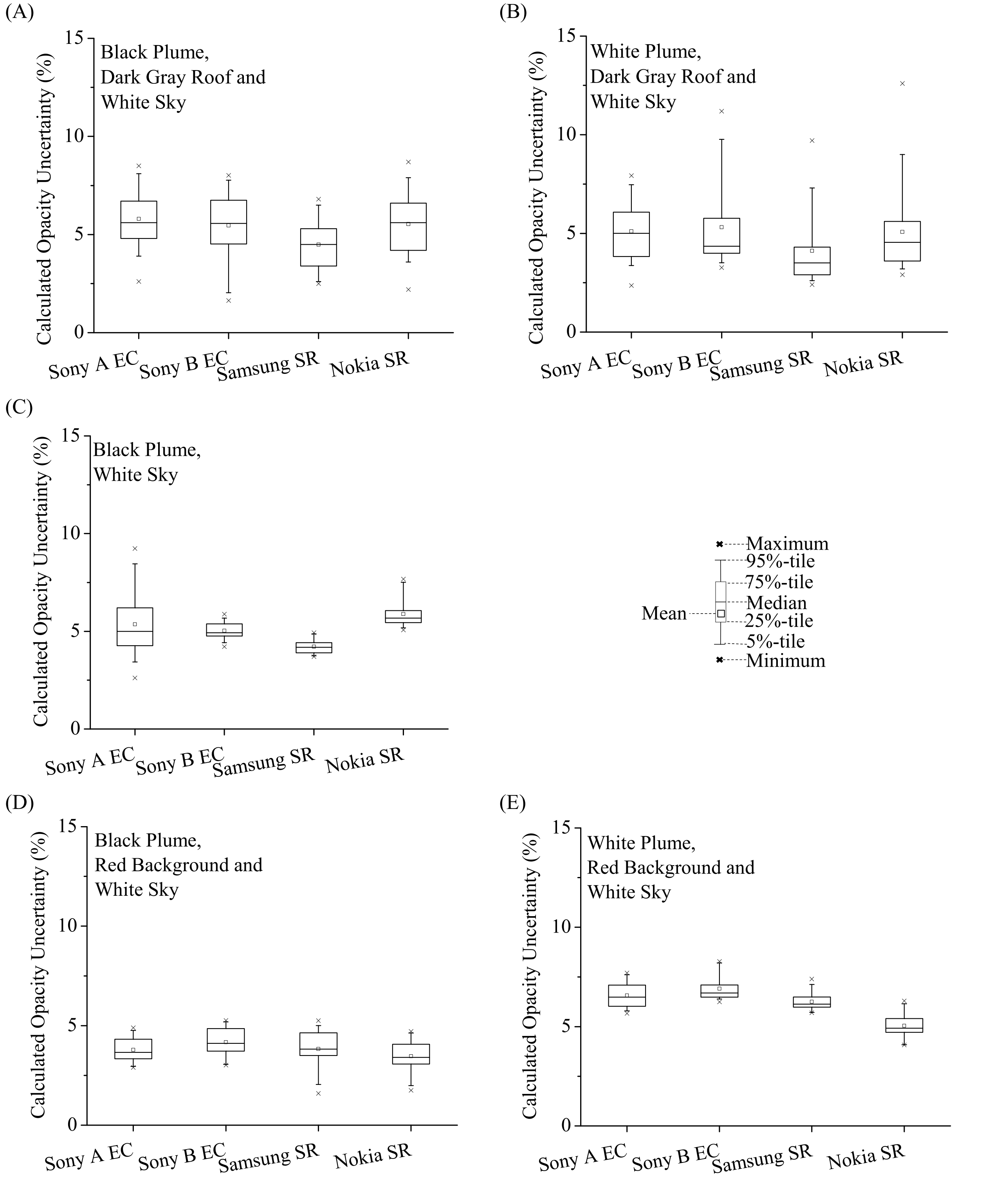

Fig. 6. Statistics of calculated opacity uncertainty in grayscale due to non-uniform background colors for (A) black plumes and (B) white plumes, using dark gray roof and white sky background pair and contrast model; (C) black plumes, using white sky background and transmission model; (D) black plumes and (E) white plumes, using red background and white sky background pair and contrast model.

background colors is 5–15% in opacity, which is higher than the uncertainty due to camera calibration (< 2%). Figs. 6(D) and 6(E) show that calculated opacity uncertainties are between 2% and 8% in opacity for black and white plumes.

The calculated DSC RGB opacity measurement uncertainties due to non-uniform background colors are shown in Fig. 7. The calculated uncertainties show that red PVs introduce the highest uncertainty (a maximum of 43%

in opacity in red PV, compared to 10% in green PV and 5% in blue PV), which is consistent with results shown in Fig. 5(A).

Analysis of Diffusive Scattering Parameter (K)

Statistics of empirical K values are displayed in Fig. 8 for each DSC, its color channels, plume colors, and backgrounds. The corresponding empirical K values are shown in Table S5 of Supporting Information. Overall, K values are smaller for black plumes than for white plumes in all DSC color PV channels. This observation is consistent with literature values for blue sky background (0.16 for black plume and 1.43 for white plume, Du, 2007). The reason is that black plumes have lower single scattering albedo (scattering to total extinction ratio). Thus, according to Eq. (3), K is smaller for black plume. The empirical K value for black plume against white sky background in grayscale is between 0.17 and 0.27 (Table S5), compared to 0.14 that is calculated from Eq. (3), 39% smaller when compared to the mean of empirical K values. As mentioned before, when the background and the plume lack contrast, K is theoretically equal to 1. The empirical K value in grayscale is between 0.80 and 0.87 for white plume against white sky, and between 0.64 and 0.89 for black plume against dark gray roof (Table S5). The theoretical value is 19% larger when compared to the mean of empirical K values for white plume against white sky, and 31% larger when compared to black plume against dark gray roof. The results show the closeness between theoretical and empirical K values when background and plume lack contrast.

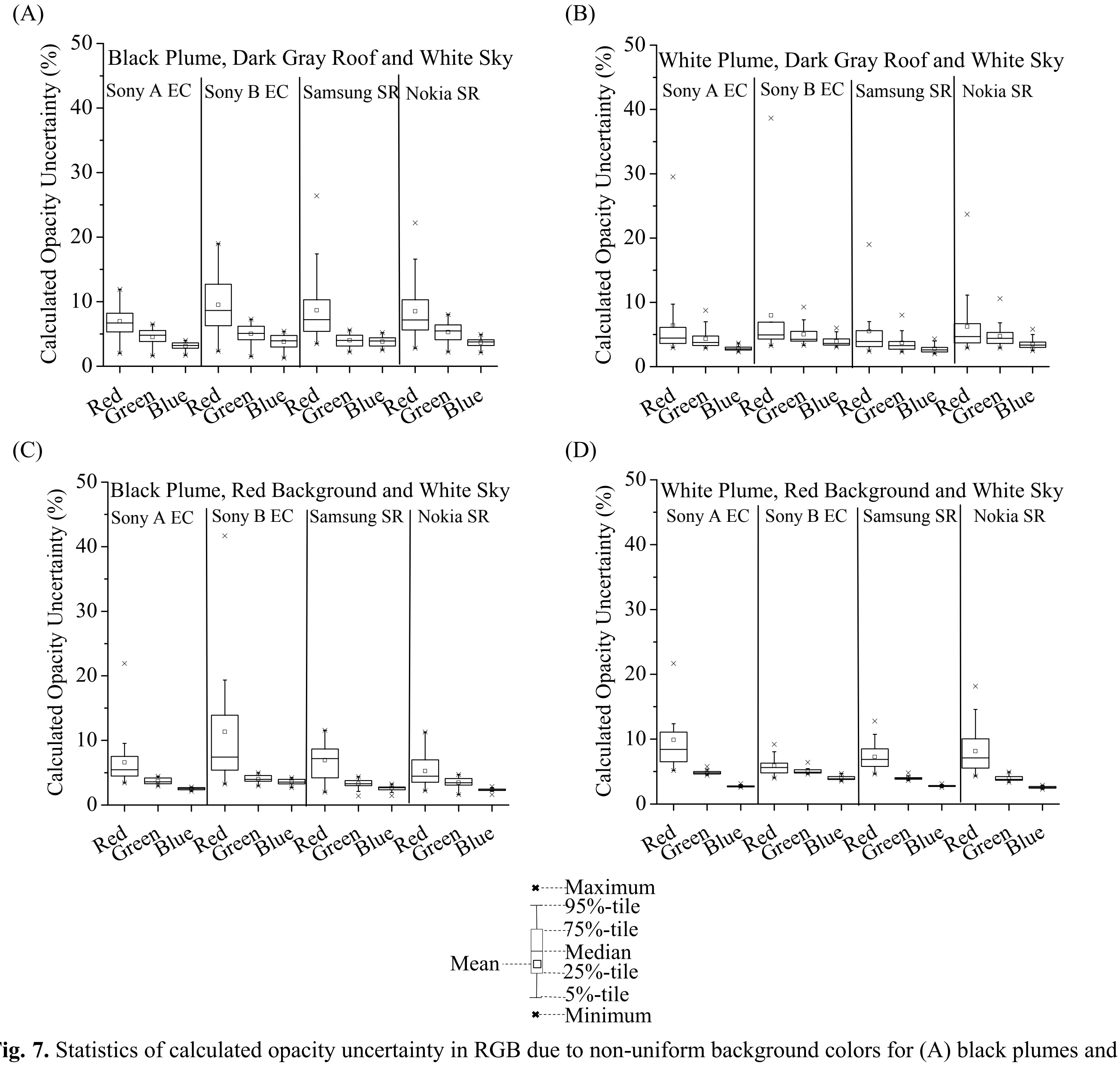

Fig. 7. Statistics of calculated opacity uncertainty in RGB due to non-uniform background colors for (A) black plumes and (B) white plumes, using dark gray roof and white sky background pair and contrast model; (C) black plumes and (D) white plumes, using red background and white sky background pair and contrast model.

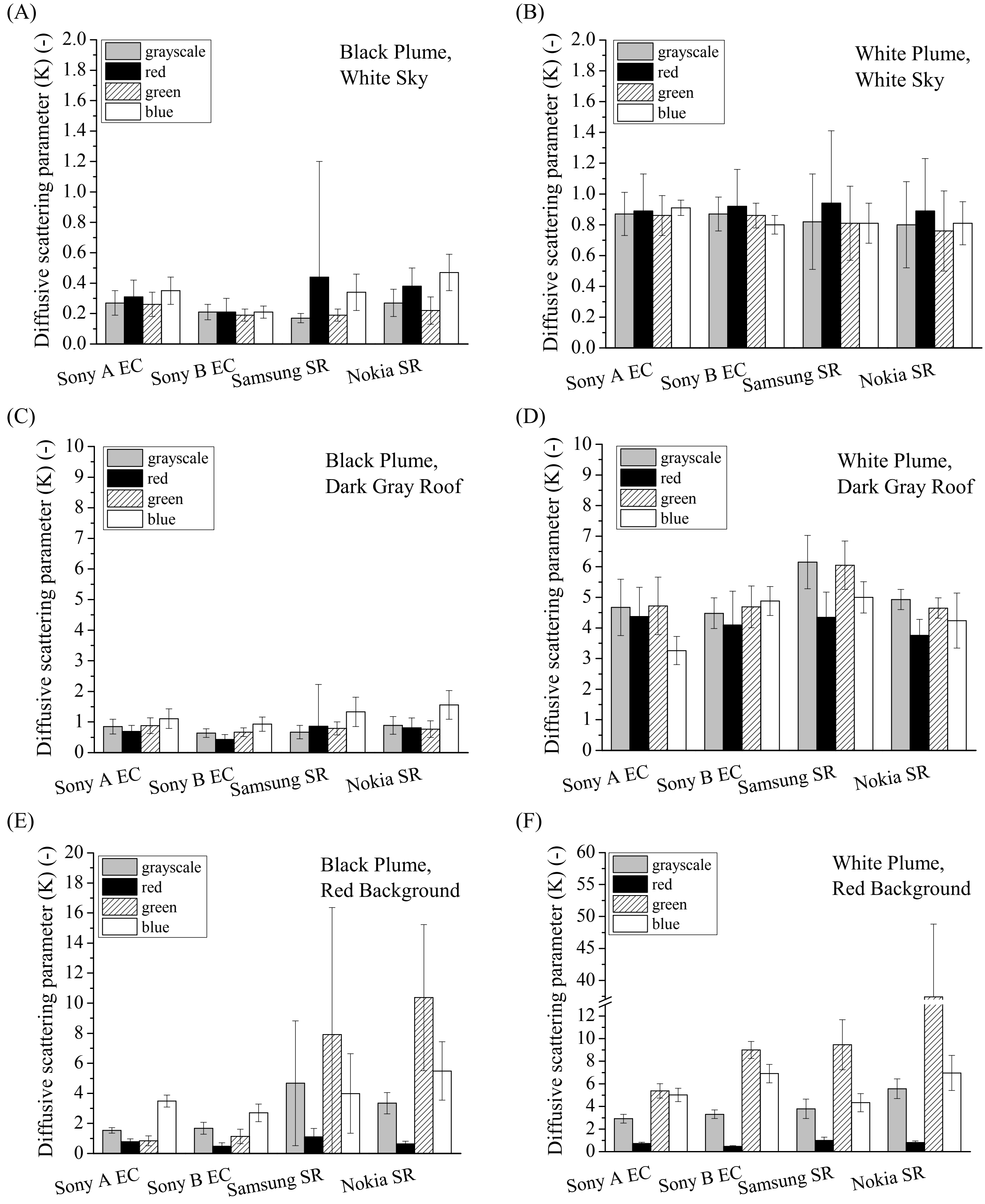

Fig. 8. Statistics of measured diffusive scattering parameters (K) for (A) black plumes and (B) white plumes, for white sky background; (C) and (D): similar to (A) and (B), but for dark gray roof background; (E) and (F): similar to (A) and (B), but for red background. Bars show means and error bars show standard deviations.

When considering wavelength dependence of K for red background, the empirically derived K values for green and blue wavelengths are 4 to 47 times larger than K values at red PV for white plumes, and 1 to 16 times higher for black plumes. A possible explanation for the smallest K for red PV with red background is that a lower background light radiance results in a higher K value based on Eq. (3). Since radiance of red light is higher than the other two colors for red background, K is the smallest for red PV. The results demonstrate that when the background color is not on grayscale, K value depends on wavelength of background color.

COVs of K values were also calculated for each background, plume color, and wavelength of measurement, in order to evaluate the uncertainty of K determined by this empirical approach. After removing COV outliers by using the 1.5 times inter-quartile range method (Montgomery and Runger, 2011), the range of COVs of K values for all grayscale, red, green, and blue measurements are 7%–38%, 13%–51%, 7%–47%, and 5%–36%, respectively. This shows that K values determined by red wavelength have the highest uncertainty.

CONCLUSIONS

Compact digital still cameras (DSCs) offer the advantage of objectivity and provide archival records compared to Method 9 human observers to quantify plume opacity values. Using smartphone DSCs offers advantages over compact DSCs including plume opacity quantification with location identification, software adaptation as a smartphone application, and wireless connectivity. This research demonstrates that the performance of smartphone DSCs on measuring plume opacity is as good as compact DSCs, by passing the Method 9 requirements. We recommend the exposure value compensation method (EC) for the calibration of automatic exposure controlled DSCs, which is simpler to use as it does not require availability of another calibrated DSC. Results show that the EC method performs as well as the previous calibration methods and introduces < 2% uncertainty, which supports the validity of the EC method. The two smartphone DSCs used in this campaign cannot be calibrated through the EC method because they are older models that do not provide exposure value compensation settings. However, recent smartphone DSCs (e.g., iPhone 6 and Samsung Galaxy S7) provide such settings, making the EC method relevant to the current smartphone DSCs.

In terms of the effects of background colors and grayscale versus RGB pixel value (PV) measurements, we observe that background contrast is a more important factor than camera calibration in determining the uncertainty of opacity measurement. Dark gray roof background against white sky provides greater contrast than red background against white sky, thus opacity uncertainty is lower. We also observe that the contrast is wavelength dependent. In this study, due to lack of contrast in red PV when considering red background against white sky background, the uncertainty in opacity measurement in red PV is higher than in green or blue PVs. Even when using dark gray roof background against white sky background, where high contrast occurs for all red, green, and blue PVs, we show that opacity values measured in green and blue PVs are less deviated from those measured in grayscale PV (3.0%), compared to red PV (7.8%). The results concerning wavelength dependency implies that when grayscale PV does not provide the greatest contrast for select backgrounds, blue or green PV can be used as alternatives in determining opacity. The wavelength dependent contrast also leads to difference in diffusive scattering parameter (K) in the transmission model, when the background color is not in grayscale.

The results have implications for future research and technology deployment. In light of future research, backgrounds with other colors (such as green trees or blue sky) should be tested to determine the wavelength dependence in opacity measurements and its uncertainty. In light of technology deployment, smartphone applications can be developed for measuring opacity using DOM, with background choices optimized to reduce uncertainty in opacity measurements.

SUPPLEMENTARY MATERIAL

Supplementary data associated with this article can be found in the online version at http://www.aaqr.org.

REFERENCES

Anenberg, S.C., Schwartz, J., Shindell, D., Amann, M., Faluvegi, G., Klimont, Z., Janssens-Maenhout, G., Pozzoli, L., Van Dingenen, R., Vignati, E., Emberson, L., Muller, N.Z., West, J.J., Williams, M., Demkine, V., Hicks, W.K., Kuylenstierna, J., Raes, F. and Ramanathan, V. (2012). Global air quality and health co-benefits of mitigating near-term climate change through methane and black carbon emission controls. *Environ. Health Perspect.* 120: 831–839.

Ångström, A. (1964). The Parameters of atmospheric turbidity. *Tellus* 1: 64–75.

ASTM Standard D7520 (2013). *Standard Test Method for Determining the Opacity of a Plume in the Outdoor Ambient Atmosphere.* ASTM International, West Conshohocken, PA.

Bevington, P.R. and Robinson, D.K. (2002). *Data Reduction and Error Analysis for the Physical Sciences,* 3rd ed. McGraw-Hill.

Conner, W.D. and Hodkinson, J.R. (1972). *Optical Properties and Visual Effects of Smoke-Stack Plumes.* Office of Air Programs Publication No. AP-30, USEPA, Washington, DC.

Dockery, D.W. and Pope, C.A. (1994). Acute respiratory effects of particulate air pollution. *Annu. Rev. Public Health* 15: 107–132.

Du, K. (2007). *Optical Remote Sensing of Airborne Particulate Matter to Quantify Opacity and Mass Emissions.* Ph.D. Dissertation, University of Illinois at Urbana-Champaign, Illinois, USA.

Du, K., Rood, M.J., Kim, B.J., Kemme, M.R., Franek, B. and Mattison, K. (2007). Quantification of plume opacity by digital photography. *Environ. Sci. Technol.* 41: 928–935.

Du, K., Wang, Y., Chen, B., Wang, K., Chen, J. and Zhang, F. (2011). Digital photographic method to quantify black carbon in ambient aerosols. *Atmos. Environ.* 45: 7113–7120.

Du, K., Shi, P., Rood, M.J., Wang, K., Wang, Y. and Varma, R.M. (2013). Digital Optical Method to quantify the visual opacity of fugitive plumes. *Atmos. Environ.* 77: 983–989.

Environment and Climate Change Canada (2010). New Source Emission Guidelines for Thermal Electricity

Generation. https://www.ec.gc.ca/lcpe-cepa/default.asp?lang=En&n=8FCC2CCB-1, Last Access: August 2016.

Hasenfratz, D., Saukh, O., Sturzenegger, S. and Thiele, L. (2012). Participatory Air Pollution Monitoring Using Smartphones. In 2nd International Workshop on Mobile Sensing, April 16–20, 2012, Beijing, China.

Illinois EPA (2015). Evaluation of Visible Emissions Course. http://www.epa.illinois.gov/topics/air-quality/smoke-school/index, Last Access: August 2016.

Jacobson, M. (2001). Global direct radiative forcing due to multicomponent anthropogenic and natural aerosols. *J. Geophys. Res.* 106: 1551–1568.

Malm, W.C. (1999). *Introduction to Visibility.* Colorado State University, Fort Collins, CO.

Montgomery, D.C. and Runger, G.C. (2011). *Applied Statistics and Probability for Engineers,* 5th ed. John Wiley & Sons, Inc.

Nieuwenhuijsen, M.J., Donaire-Gonzalez, D., Rivas, I., De Castro, M., Cirach, M., Hoek, G., Seto, E., Jerrett, M. and Sunyer, J. (2015). Variability in and agreement between modeled and personal continuously measured black carbon levels using novel smartphone and sensor technologies. *Environ. Sci. Technol.* 49: 2977–2982.

Poduri, S., Nimkar, A. and Sukhatme, G.S. (2010). Visibility Monitoring Using Mobile Phones. http://robotics.usc.edu/~mobilesensing/visibility/MobileAirQualitySensing.pdf, Last Access: August 2016.

Pollution Control Department (2004). Thai Environmental Regulations - Air Quality and Noise Standards. http://www.pcd.go.th/info_serv/en_reg_std_airsnd03.html, Last Access: August 2016.

Pope, C. and Dockery, D. (2006). Health effects of fine particulate air pollution: Lines that connect. *J. Air Waste Manage. Assoc.* 56: 709–742.

Ramanathan, N., Lukac, M., Ahmed, T., Kar, A., Praveen, P.S., Honles, T., Leong, I., Rehman, I.H., Schauer, J.J. and Ramanathan, V. (2011). A Cellphone based system for large-scale monitoring of black carbon. *Atmos. Environ.* 45: 4481–4487.

Reis, S., Seto, E., Northcross, A., Quinn, N.W.T., Convertino, M., Jones, R.L., Maier, H.R., Schlink, U., Steinle, S., Vieno, M. and Wimberly, M.C. (2015). Integrating modelling and smart sensors for environmental and human health. *Environ. Modell. Software* 74: 238–246.

Snyder, E.G., Watkins, T.H., Solomon, P.A., Thoma, E.D., Williams, R.W., Hagler, G.S.W., Shelow, D., Hindin, D.A., Kilaru, V.J. and Preuss, P.W. (2013). The changing paradigm of air pollution monitoring. *Environ. Sci. Technol.* 47: 11369–11377.

USEPA (1993). *Visible Emissions Field Manual EPA Methods 9 and 22.* Office of Air Quality Planning and Standards, Washington, DC.

USEPA (2016). National Ambient Air Quality Standards (NAAQS). https://www.epa.gov/criteria-air-pollutants/naaqs-table, Last Access: August 2016.

Vahlsing, C. and Smith, K.R. (2012). Global review of national ambient air quality standards for PM_{10} and SO_2 (24 h). *Air Qual. Atmos. Health* 5: 393–399.

Watson, J.G. (2002). Visibility: Science and Regulation. *J. Air Waste Manage. Assoc.* 52: 628–712.

WHO (2006). *WHO Air Quality Guidelines for Particulate Matter, Ozone, Nitrogen Dioxide and Sulfur Dioxide.* WHO Press, Geneva, Switzerland.

Received for review, August 24, 2016
Revised, November 30, 2016
Accepted, December 21, 2016